# Insulin resistance in skeletal muscles of caveolin-3-null mice

**Jin Oshikawa*, Koji Otsu*, Yoshiyuki Toya*, Takashi Tsunematsu*, Raleigh Hankins†, Jun-ichi Kawabe‡, Susumu Minamisawa*, Satoshi Umemura*, Yasuko Hagiwara§, and Yoshihiro Ishikawa*‡¶**

*Departments of Physiology and Medicine, Yokohama City University School of Medicine, 3-9 Fukuura Kanazawa, Yokohama 236-0004, Japan; †Health Sciences Research Institute, Incorporated, 106 Godocho Hodogaya, Yokohama 240-0005, Japan; §National Institute of Neuroscience, 4-1-1 Ogawahigashicho Kodaira, Tokyo 187-8502, Japan; and ‡Department of Cell Biology and Molecular Medicine and Department of Medicine (Cardiology), New Jersey Medical School, University of Medicine and Dentistry of New Jersey, 185 South Orange Avenue, Newark, NJ 07103

Edited by C. Ronald Kahn, Harvard Medical School, Boston, MA, and approved July 14, 2004 (received for review March 23, 2004)

**Type 2 diabetes is preceded by the development of insulin resistance, in which the action of insulin is impaired, largely in skeletal muscles. Caveolin-3 (Cav3) is a muscle-specific subtype of caveolin, an example of a scaffolding protein found within membranes. Cav is also known as growth signal inhibitor, although it was recently demonstrated that the genetic disruption of Cav3 did not augment growth in mice. We found, however, that the lack of Cav3 led to the development of insulin resistance, as exemplified by decreased glucose uptake in skeletal muscles, impaired glucose tolerance test performance, and increases in serum lipids. Such impairments were markedly augmented in the presence of streptozotocin, a pancreatic $\beta$ cell toxin, suggesting that the mice were susceptible to severe diabetes in the presence of an additional risk factor. Insulin-stimulated activation of insulin receptors and downstream molecules, such as IRS-1 and Akt, was attenuated in the skeletal muscles of Cav3 null mice, but not in the liver, without affecting protein expression or subcellular localization. Genetic transfer of Cav3 by needle injection restored insulin signaling in skeletal muscles. Our findings suggest that Cav3 is an enhancer of insulin signaling in skeletal muscles but does not act as a scaffolding molecule for insulin receptors.**

Diabetes mellitus comprises a group of common metabolic disorders that share the phenotype of hyperglycemia (1). In particular, adult-onset diabetes, or type 2 diabetes, is a heterogeneous group of disorders usually characterized by varying degrees of insulin resistance and increased blood glucose concentrations. Insulin binding to insulin receptors (IR) evokes a cascade of phosphorylation events, as commonly seen in other growth factor signaling, beginning with the autophosphorylation of IR in multiple tyrosyl residues, followed by downstream signaling events (2). The combined actions of these events mediate the biological effects of insulin, leading to increased glucose uptake.

Caveolin (Cav) is a major protein component of caveolae, flask-shaped plasma membrane invaginations found in myocytes, endothelial cells, fibroblasts, and adipocytes (for review, see ref. 3). Numerous studies have indicated that Cav works as a scaffolding molecule; it binds directly to various receptors and their effector molecules and anchors these molecules to the caveolae. More important, Cav inhibits the function of these molecules. Cav-1 (Cav1)-mediated inhibition, by the use of a short stretch of the amino terminus domain of Cav (or the Cav scaffolding domain peptide), has been demonstrated with various kinases involved in cellular growth, such as receptor tyrosine kinases, e.g., epidermal growth factor-R (4) or platelet-derived growth factor-R (5), as well as protein kinase C (6) or Src (7). These studies have demonstrated that the Cav1 peptide directly bound to these molecules and inhibited their activity. Accordingly, it is now believed that Cav1 is an inhibitor of cellular growth signal (8–10).

Cav3 is the newest member of the Cav family (11). Cav3, a muscle-specific subtype, forms a complex with dystrophin and its associated glycoproteins that are specific to muscle cells (12). Although Cav3 is localized to sarcolemmic caveolae in adults, it is associated with the developing T tubule system during skeletal muscle maturation (13). Cav3 has a high amino acid sequence homology to Cav1 (12) and thus may play a role similar to Cav1 in inhibiting growth signal (6). However, a recent study demonstrated that mice with the disrupted Cav3 gene (Cav3 knockout, Cav3KO) had no acceleration in growth (14). Mice with the disrupted Cav1 gene, on the contrary, exhibited a lean body mass, most likely due to a decrease in the stability of IR protein (15), suggesting that Cav1 does not inhibit growth *in vivo* but regulates insulin signaling by keeping the stability of IR protein.

Because we previously demonstrated that a Cav3 peptide potently and directly stimulated IR kinase activity *in vitro* (16), and the role of Cav may differ between Cav1 and Cav3, as exemplified by distinctive ontogenic changes (17), we are interested in the role of Cav3 in regulating insulin signaling. In particular, we have examined the impact of disrupting Cav3 on insulin signaling *in vivo* in skeletal muscles, a major organ responsible for glucose uptake. We demonstrate the attenuation of insulin signal and the development of insulin resistance, but no major changes in the protein expression of IR or its subcellular localization.

## Materials and Methods

**Development of Cav3KO Mice.** Cav3KO were originally developed as a model of muscular dystrophy, because Cav3 anchors and stabilizes the dystrophin complex formation. This abnormality becomes apparent in late developmental stages, but the mice showed no growth abnormalities (14). In this study, 10- to 12-week-old Cav3KO mice, their WT littermates, Cav3KO mice that had been backcrossed to C57BL/6 for 10 generations, and C57BL/6 were used. The animals were maintained in accordance with the guidelines of the animal experiment committees of Yokohama City University School of Medicine and New Jersey Medical School.

**Immunoblotting.** For immunoblotting of Cav, tissues lysates from the skeletal muscle were prepared in a lysis buffer containing 50 mM Tris·HCl (pH 8.0), 2 mM EGTA, 1% SDS, and protease inhibitors. After adjusting the protein concentration, the samples were separated by SDS/PAGE and transferred to poly(vinylidene difluoride) membrane. The membranes were incubated with specific primary antibodies against Cav1, -2, and -3 (BD Biosciences, Palo Alto, CA) or PTP1B (Upstate Biotechnology, Lake Placid, NY), followed by visualization using horseradish peroxidase-conjugated specific secondary antibodies. All immu-

This paper was submitted directly (Track II) to the PNAS office.

Abbreviations: Cav, caveolin; Cav*n*, Cav-*n*; Cav3KO, Cav3 knockout; IR, insulin receptor; IRS, IR substrate; PI3K, phosphatidylinositol 3-kinase; STZ, streptozotocin; IR$\beta$, IR$\beta$ subunit; IRS-1, IR substrate-1.

¶To whom correspondence should be addressed. E-mail: ishikayo@umdnj.edu.





www.pnas.org/cgi/doi/10.1073/pnas.0402053101

noreactive bands were detected by SuperSignal substrate kit (Pierce) and analyzed by densitometry.

**Immunoprecipitation Assays.** An *in vivo* phosphorylation assay of the IR$\beta$ subunit (IR$\beta$) or IR substrate-1 (IRS-1) was performed as described (18), with some modifications. After fasting for 16 h, mice were anesthetized with an i.p. injection of pentobarbital (100 mg/kg). Insulin was injected (5 milliunits/g) through the inferior vena cava, followed by decapitation after 2 min. Tissues (soleus muscles and liver) were quickly harvested and stored in liquid $N_2$. These tissues were lysed in a lysis buffer containing 25 mM Tris·HCl (pH 8.0), 10 mM EGTA, 10 mM EDTA, 10 mM $Na_4P_2O_7$, 100 mM NaF, 10 mM $Na_3VO_4$, 1% Nonidet P-40, and protease inhibitors at 4°C for 30 min. After removing debris and adjusting the protein concentrations, tissue lysates were subject to immunoprecipitation using polyclonal antibodies to IR$\beta$ (BD Biosciences) or IRS-1 (Upstate Biotechnology) for 12 h. Immune complexes were formed by incubation with Protein G Sepharose (Amersham Pharmacia Biosciences) for 2 h. The immune complexes were washed with a washing buffer containing 25 mM Tris·HCl (pH 8.0), 10 mM EGTA, 10 mM EDTA, 10 mM $Na_4P_2O_7$, 100 mM NaF, 10 mM $Na_3VO_4$, 0.1% Nonidet P-40, and protease inhibitors three times, solubilized, and subject to immunoblotting. To analyze the phosphorylation of IR$\beta$ and IRS-1, immunoblotting was performed after immunoprecipitation by using antibodies against phosphortyrosine (BD Biosciences). Coimmunoprecipitation assays for IRS-1 and phosphatidylinositol 3-kinase (PI3K)p85 were performed similarly by using IRS-1 and PI3Kp85 (Upstate Biotechnology) antibodies. Phosphorylated PKB/Akt was quantitated with immunoblotting by the use of an antiphospho-serine$^{473}$-Akt/PKB antibody (Promega). Coimmunoprecipitation assays for IR$\beta$ and Cav3 were performed by the use of caveolar fractions (fractions 4–6) after the sucrose gradient fractionation of skeletal (soleus) muscle tissues (19).

**Protein Fractionation by the Sucrose Gradient Method.** Caveolae fractions were separated by the sodium carbonate-based detergent-free method (16). Briefly, skeletal muscle tissues (400 mg) were homogenized in a solution containing 0.5 M sodium carbonate (pH 11) and protease inhibitors with three 10-s bursts of a Polytron tissue grinder (Kinematica, Lucerne, Switzerland) and four 20-s bursts of a sonicator. The homogenates were adjusted to 45% sucrose by adding 90% sucrose in a buffer containing 25 mM Mes (pH 6.5) and 0.15 M NaCl and placed at the bottom of an ultracentrifugation tube. A 5–35% discontinuous sucrose gradient was formed above and centrifuged at 39,000 rpm at 4°C for 16 h in a Beckman SW-41Ti rotor. From the top of the tube, 13 fractions were collected. Caveolae fractions were accumulated in fractions 4–6. These fractions contained $<5\%$ of total tissue protein content. To analyze the intracellular localization of IR$\beta$ or PTP1B, an equal volume from each fraction was subjected to immunoblotting.

**RNA Extraction and Northern Blot Analysis.** To detect the mRNA expression of IR$\beta$, total RNA was extracted from the soleus muscle of WT and Cav3KO mice. Total RNA was separated by agarose gel and transferred to a nylon membrane. The mRNA expression of IR$\beta$ was detected by hybridization to a $^{32}$P-labeled probe generated from a mouse IR$\beta$ cDNA.

**Streptozotocin (STZ) Treatment.** STZ treatment was performed on the overnight-fasted mice (20). STZ was dissolved with saline containing 0.05 M citrate and injected i.p. at a dose of 100 mg/kg. The analysis of blood glucose and insulin concentration was performed 2 weeks after STZ injection.

**Glucose Uptake Assay.** After fasting and anesthesia (21, 22), the soleus muscles were quickly harvested, followed by incubation at 30°C for 30 min in a Krebs–Ringer Bicarbonate (KRB) buffer solution containing 5 mM Hepes (pH 7.4), 0.1% BSA, and 2 mM pyruvate in the presence or absence of insulin, continuously gassed with 95% $O_2$ and 5% $CO_2$. The solution was then aspirated and the muscles reincubated in a KRB buffer solution containing 8 mM [$^3$H]2-deoxyglucose and 32 mM [$^{14}$C]mannitol in the presence or absence of insulin for 30 min at 30°C. The muscles were then quickly frozen in liquid $N_2$ until use. The muscles were lysed with 1 M NaOH at 70°C for 30 min, followed by centrifugation at 12,000 $\times$ *g* for 10 min. The supernatant was neutralized with 1 M HCl, followed by the determination of radioactivity for [$^3$H]2-deoxyglucose and [$^{14}$C]mannitol by a scintillation counter. Net uptake of glucose was determined by subtracting the amount of [$^{14}$C]mannitol from that of [$^3$H]2-deoxyglucose.

**Glucose Tolerance Test.** After 16-h fasting, glucose (2 mg/g of body weight) was injected i.p. Blood glucose concentration was determined 0, 30, 60, 90, and 120 min after injection of glucose by the use of a glucometer. To measure the serum insulin concentration, blood was obtained from the orbita and clotted, and serum was extracted. Serum insulin concentration was measured at 0, 15, and 30 min after injection of glucose by the use of the Insulin Ultrasensitive ELISA Kit (Mercodia, Uppsala).

**Measurements of Serum Lipids.** Blood samples were obtained from fasted mice (16 h) through the orbita and were subject to the determination of serum concentrations of free fatty acids, triglycerides, and total cholesterol. Total cholesterol and triglycerides were determined by use of a commercial kit (Kyowa Medex, Tokyo), and free fatty acids were determined by use of a kit from Shino-Test (Tokyo).

**Adenovirus Construction.** For construction of adenoviral vectors, full-length cDNA-encoding rat Cav3 was cloned into the shuttle vector for construction of adenoviral vector harboring Cav3 by using an AdenoX adenovirus construction kit (Clontech). Adenovirus-mediated transduction was performed as described (23). As a control study, adenovirus vector harboring GFP was used. All experiments were performed 48 h after transduction.

**Adenovirus Injection.** We injected $2 \times 10^8$ plaque-forming units of the adenovirus containing the *Cav3* gene into the soleus muscle of Cav3KO mice (24). Control experiments were performed by using adenovirus-harboring GFP. At 2 days after injection, insulin was injected through the inferior vena cava, followed by removal of the muscle tissues for immunoprecipitation assays to detect the phosphorylation of IR$\beta$ and IRS-1.

## Results

**Changes in IR Signal in Cav3KO.** If Cav3 inhibits insulin signaling, as already demonstrated for many other growth factor signals, the disruption of Cav3 would enhance insulin signaling *in vivo*. We found, however, that IR$\beta$ in the skeletal muscle of Cav3KO was unchanged from that of WT at basal but was significantly lower in Cav3KO upon insulin stimulation (Fig. 1*A*). Similarly, IRS-1 phosphorylation was similar between Cav3KO and WT at basal but was lower by half in Cav3KO after insulin stimulation (Fig. 1*B*). PI3Kp85 is an additional downstream molecule involved in insulin signaling that associates with IRS-1. The association of IRS-1 with PI3Kp85 was also decreased after insulin stimulation in Cav3KO (Fig. 1*C*). Phosphorylation of Akt/PKB was also decreased to an even greater degree in Cav3KO upon insulin stimulation (Fig. 1*D*). These findings indicated that insulin signaling in the skeletal muscle of Cav3KO

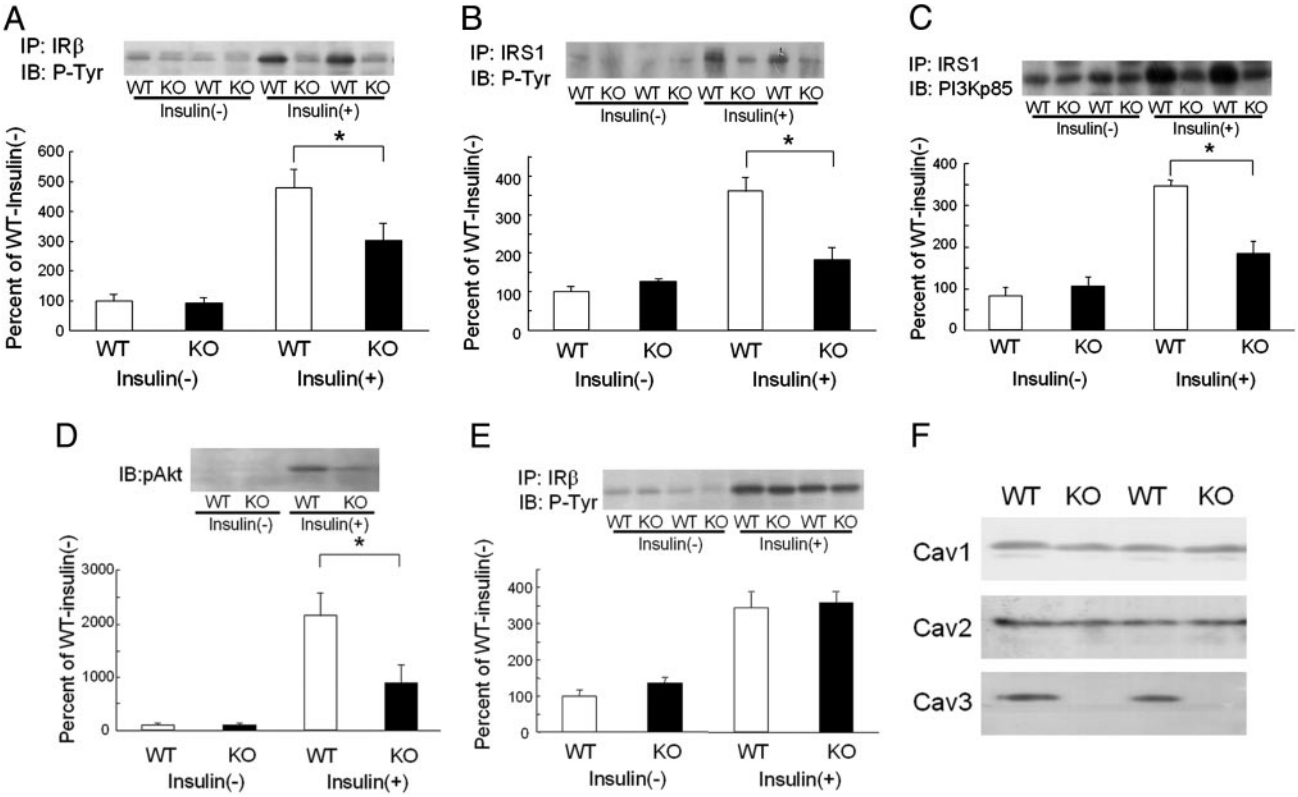


**Fig. 1.** Decreased insulin signaling in skeletal muscle tissues of Cav3KO. Two minutes after insulin injection, tissues were harvested to determine insulin signaling in WT (WT) and Cav3KO (KO). (*A*) Phosphorylation of IR$\beta$ in skeletal muscles was quantitated by immunoblotting with a phosphotyrosine antibody (IB*:* P-Tyr) after immunoprecipitation with an IR$\beta$ antibody (IP: IR$\beta$) in the absence [insulin(−)] or presence [insulin(+)] of insulin stimulation. *, $P < 0.05$ relative to WT; $n = 8$. (*Inset*) A representative photo. (*B*) Phosphorylation of IRS-1 was quantitated by immunoblotting with a phosphotyrosine antibody after immunoprecipitation with an IRS-1 antibody (IP*:* IRS1) in the absence or presence of insulin stimulation. *, $P < 0.05$ relative to WT, $n = 8$. (*Inset*) A representative photo. (*C*) PI3Kp85, coimmunoprecipitated with IRS-1, was quantitated by immunoblotting with a PI3Kp85 antibody (IB*:* PI3Kp85) after immunoprecipitation with an IRS-1 antibody (IP*:* IRS1) in the absence or presence of insulin stimulation. *, $P < 0.05$ relative to WT, $n = 8$. (*Inset*) A representative photo. (*D*) Phosphorylation of Akt1/PKB was quantitated by immunoblotting with an antiphospho-serine$^{473}$-Akt1/PKB antibody (IB*:* pAkt) in the absence or presence of insulin stimulation. *, $P < 0.05$ relative to WT, $n = 4$. (*Inset*) A representative photo. (*E*) Phosphorylation of IR$\beta$ in the liver was quantitated by immunoblotting with a phosphotyrosine antibody (IB*:* P-Tyr) after immunoprecipitation with an IR$\beta$ antibody (IP*:* IR$\beta$) in the absence or presence of insulin stimulation. (*Inset*) A representative photo. (*F*) Expression of Cav1, Cav2, and Cav3 in skeletal muscles was compared between WT and Cav3KO by immunoblotting.

was significantly lower than in WT upon insulin stimulation, suggesting that Cav3 acts as an enhancer of insulin signaling in WT.

The above findings contrast with the fact that Cav usually inhibits growth factor signals (3) but rather agrees with our previous study in which a Cav3-derived peptide directly activated IR kinase activity *in vitro* (16). We also examined changes in insulin signaling in the liver, where Cav3 expression is absent in both WT and Cav3KO. There was no difference between Cav3KO and WT in insulin-stimulated phosphorylation of IR$\beta$ (Fig. 1*E*) and IRS as well as the association of PI3Kp85 with IRS-1 (data not shown), suggesting that the impairment of insulin signaling in Cav3KO occurred only in muscles. Expression of other Cav subtypes (Cav1 and Cav2) was unchanged in skeletal muscles (Fig. 1*F*).

**Expression of IR and Its Related Molecules Was Unchanged.** Impairment of insulin action can be induced by changes in the activity and/or expression of the molecules involved in insulin signaling, as proposed in various transgenic models (25–27). Indeed, a very recent study demonstrated that Cav1 disruption led to decreased stability of Cav1 protein and therefore its expression (15). We examined changes in the expression of IR and other molecules involved in insulin signaling in the skeletal muscles of Cav3KO. The protein expression of IR$\beta$, IRS-1, or PI3K was not altered in Cav3KO relative to WT (Fig. 2*A*). The mRNA expression of IR$\beta$ was not altered in Cav3KO (Fig. 2*B*). The expression of PTP1B, a major phosphatase involved in insulin signaling, as well as that of Grb and Shc, intermittent molecules in insulin and other growth factor signals, was unchanged (data not shown). Although IR$\beta$ and Cav3 were coimmunoprecipitated (Fig. 2*C*), as suggested previously (16), the disruption of Cav3 did not alter the subcellular localization of IR$\beta$ in Cav3KO, as determined by sucrose gradient fractionation (Fig. 2*D*). Similarly, subcellular localization of PTP1B was not altered (Fig. 2*E*). Together with these findings, our findings strongly suggest that insulin action was impaired at the point of IR$\beta$ activity in Cav3KO. However, we do not exclude the possibility that Cav3 may inhibit the action of a putative inhibitor(s) of insulin signal, and that the disruption of Cav3 has dislocated such inhibitors from the site of IR in Cav3KO.

**Impaired Glucose Uptake in the Muscles of Cav3KO Mice.** We next examined whether glucose uptake, a final output of IR stimulation, was disturbed in Cav3KO. We found that the uptake of glucose was markedly decreased in the skeletal muscle of Cav3KO (Fig. 3*A*). Glucose uptake in the soleus muscles at basal was not significantly different between Cav3KO and WT but was significantly decreased (≈60%) upon insulin stimulation, suggesting impairment of insulin-stimulated glucose uptake in

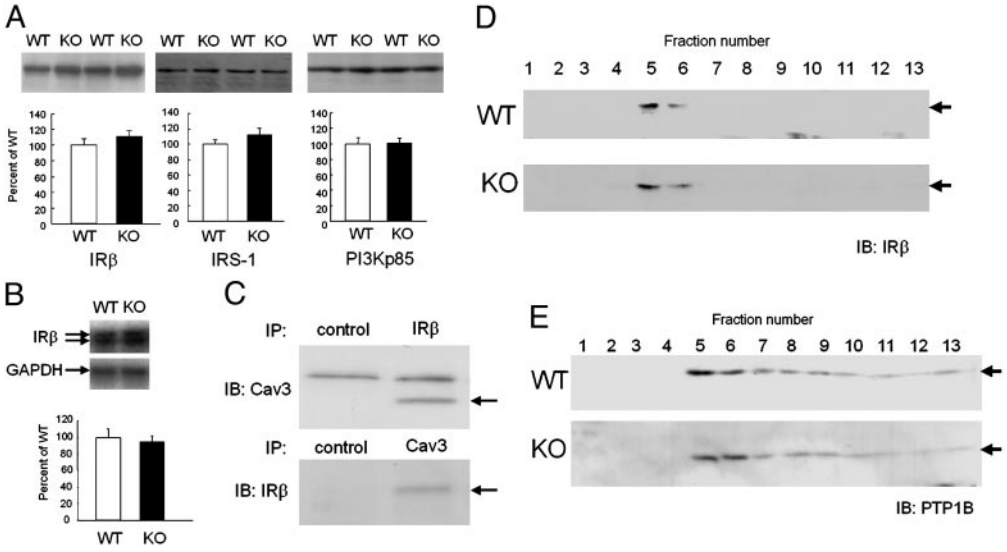


**Fig. 2.** Unaltered expression and subcellular localization of IR$\beta$ and its related molecules in Cav3KO. (*A*) Protein expression of IR$\beta$, IRS-1, and P13Kp85 in soleus muscle tissues of WT (WT, open bars) and Cav3KO (KO, filled bars). Means ± SEM are shown. $n = 8$. (*Insets*) Representative photos. (*B*) mRNA expression of IR$\beta$ in soleus muscle tissues of WT and Cav3KO. GAPDH was used as loading control. Means ± SEM are shown. $n = 8$. (*Inset*) A representative photo. (*C*) Coimmunoprecipitation assays of Cav3 and IR$\beta$. The caveolar fractions from soleus muscle tissues were used for coimmunoprecipitation assays (IP) by using IR$\beta$ and Cav3 antibodies, followed by immunodetection (IB) of Cav3 (*Upper*) and IR$\beta$ (*Lower*), respectively. Arrows indicate Cav3 (*Upper*) and IR$\beta$ (*Lower*). Nonimmune mouse and rabbit IgGs were used as control. (*D* and *E*) Subcellular localization of IR$\beta$ (*D*) or PTP1B (*E*) in soleus muscle tissues of WT (WT) and Cav3KO (KO). After sucrose gradient centrifugation, IR$\beta$ or PTP1B was detected by immunoblotting (arrows).

Cav3KO. When the glucose tolerance test was performed to the same amount of glucose administered, blood glucose levels remained at a higher level in Cav3KO, in particular 90–120 min after glucose administration (Fig. 3*B*), indicating that the clearance of glucose was impaired. This alteration in glucose metabolism was most likely due to the impairment of glucose uptake by peripheral muscles and not by the alteration in insulin secretion, because serum insulin concentrations were similar between WT and Cav3KO in both the fasting and glucose-loaded states (Fig. 3*C*).

STZ, a pancreatic $\beta$ cell toxin, can induce impairment of pancreatic function and lower peripheral insulin sensitivity (20). Cav3KO and WT were treated similarly by i.p. injection of STZ (100 mg/kg), and the glucose tolerance test was performed 2 weeks later. The fasting blood glucose was markedly elevated in Cav3KO, whereas it was only modestly elevated in WT. The glucose tolerance test demonstrated that glucose levels were increased and remained at much higher levels in Cav3KO than in WT at any time points (Fig. 3*D*), suggesting that Cav3KO mice, which were in a state of insulin resistance, were susceptible to severe diabetes in the presence of an additional risk factor, reminiscent of human type 2 diabetes.

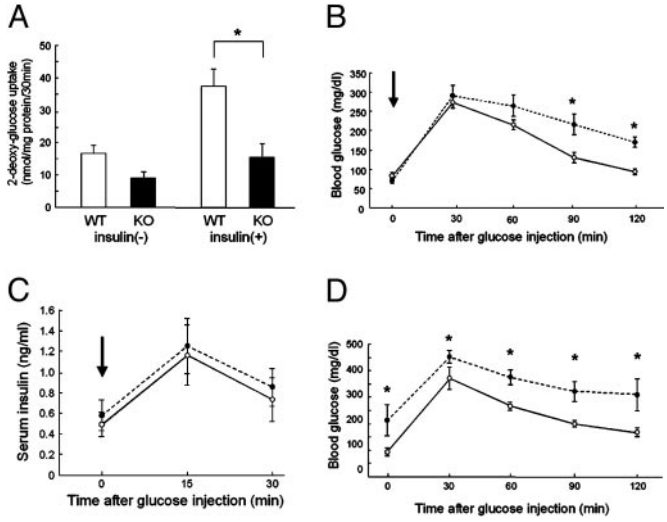


**Fig. 3.** Impaired insulin signaling in Cav3KO. (*A*) Glucose uptake in skeletal muscles. 2-Deoxy-D-[1,2-$^3$H]glucose (2-DG) uptake into soleus muscles was measured for 30 min. The muscle samples from WT (open bars, WT) and Cav3KO (filled bars, KO) were incubated in the absence [insulin(-)] or presence [insulin(+)] of insulin (14 nM), followed by measurements of 2-DG uptake. Means ± SEM are shown. *, $P < 0.05$ relative to WT; $n = 4$. (*B*) Blood glucose levels in glucose tolerance test. Glucose (2 g/kg) was administered i.p., and blood glucose levels were determined 0, 30, 60, 90, and 120 min after injection. Open circles, WT; filled circles, Cav3KO. Arrow indicates the time of glucose injection. *, $P < 0.05$ relative to WT; $n = 8$. (*C*) Blood insulin levels after glucose injection. Insulin concentrations were similarly determined at 0, 15, and 30 min after glucose injection. $n = 8$. (*D*) Blood glucose levels in glucose-tolerance test in STZ-treated mice. STZ (100 mg/kg) was administered to WT (open circles) and Cav3KO (filled circles), and the glucose tolerance test was performed after 2 weeks. *, $P < 0.05$ relative to WT, $n = 4$.

**Lipid Metabolism Was Also Impaired.** Development of insulin resistance in Cav3KO was accompanied by abnormal lipid metabolism. Fasting triglyceride concentrations showed the greatest degree of elevation: Cav3KO had levels more than twice those

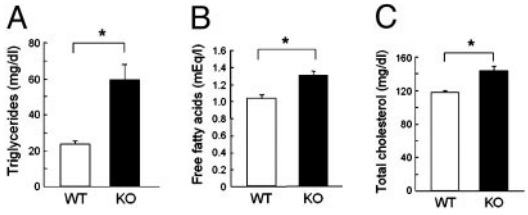


**Fig. 4.** Increased serum lipids in Cav3KO. Serum was obtained from overnight-fasted mice and measured for triglycerides (*A*), free fatty acids (*B*), and total cholesterol (*C*). Open bars, WT (WT); filled bars, Cav3KO (KO). Means ± SEM are shown. *, $P < 0.05$ relative to WT, $n = 8$.

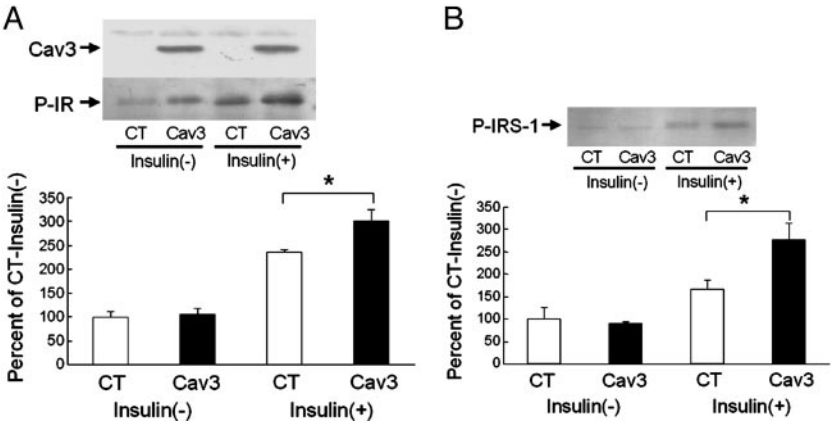


**Fig. 5.** Increased insulin signaling in skeletal muscle tissues by Cav3 gene transfer. Adenovirus harboring either Cav3 or GFP as control was injected into soleus muscles of Cav3KO. Insulin was given intravenously 48 h after injection, and soleus muscles were harvested for immunoprecipitation and immunoblotting assays. (*A*) Phosphorylation of IR$\beta$ (P-IR) was quantitated by phosphotyrosine antibody after immunoprecipitation in the absence [insulin(−)] or presence [insulin(+)] of insulin stimulation between control (CT) and Cav3 injection (Cav3). Means ± SEM are shown. *, $P < 0.05$ relative to WT; $n = 6$. (*Insets*) A representative photo of the expression of Cav3 in soleus muscles (*Upper*) and of the phosphorylation of IR$\beta$ in the presence or absence of insulin (*Lower*). (*B*) Phosphorylation of IRS-1 was quantitated by phosphotyrosine antibody after immunoprecipitation in the absence or presence of insulin stimulation between control and Cav3 injection. *, $P < 0.05$ relative to WT; $n = 6$. (*Inset*) A representative photo of the phosphorylation of IRS-1 (P-IRS-1) in the presence or absence of insulin.

of WT. Fasting free fatty acid and total cholesterol concentrations were also elevated in Cav3KO, although to a lesser but still significant degree relative to triglyceride concentrations (Fig. 4). These findings are consistent with those in the human insulin-resistant state, suggesting that Cav3KO have features of the insulin-resistant syndrome.

**Genetic Transfer of Cav3 Improved Insulin Signaling.** The above findings suggest that Cav3 plays a role in insulin signaling as an enhancer *in vivo*, most likely at the level of IR (16). If this is the case, overexpression of Cav3 should increase and restore insulin signaling in Cav3KO. In the same way that diabetic patients receive insulin injections, we injected Cav3, but intramuscularly, to enhance insulin signaling in Cav3KO. Cav3 genes were delivered to the skeletal muscles of Cav3KO by the use of an adenovirus vector, leading to a modest degree of overexpression of Cav3 in muscles (Fig. 5*A*). We found that this was sufficient to increase insulin-stimulated phosphorylation of IR$\beta$ (Fig. 5*A*), suggesting that Cav3 enhanced IR signaling in Cav3KO. The activation of IRS-1 by insulin was also increased 60% (Fig. 5*B*), strongly suggesting that Cav3 is an enhancer of insulin signaling, most likely through direct activation of IR$\beta$ in a synergistic manner with insulin.

## Discussion

The above findings are consistent with the concept that Cav3 enhances insulin signaling at the level of IR, most likely through direct stimulation of IR kinase activity (16). Insulin secretion from the pancreas was intact in Cav3KO, but insulin signaling was reduced in the muscles, although not in the liver, another major target organ of insulin. Cav3KO also exhibited hyperlipidemia. Overall, this phenotype is similar to that reported in muscle-specific IR knockout mice (26, 28).

Although IR is well known as an essential molecule involved in insulin signaling, Cav has been poorly recognized as a key molecule within the same signaling process. Instead, Cav is known as a general growth signal inhibitor. It was initially proposed that insulin stimulates tyrosine phosphorylation of Cav1, although the functional significance of this finding remained unclear (29). More recently, several investigators, including ourselves, independently demonstrated that IR is found in the same microdomain as Cav1 in adipocytes or hepatic cells (16, 30, 31), despite the fact that other molecules involved in insulin signaling, such as GLUT4 and PI3K, were not found in the same microdomain (32–34), implicating the presence of physical and/or functional interaction between Cav and IR. Subsequently, it was demonstrated that the overexpression of Cav1 enhanced insulin signaling in COS cells, but this enhancement was absent or even reversed in adipocytes (35), suggesting that Cav1 can regulate insulin signaling, but that the Cav1 effect varies among cell types. We have shown that, by the use of Cav scaffolding domain peptides, Cav1 can stimulate the kinase activity of IR, but Cav3 can do so to a much greater degree *in vitro* (16), suggesting that the effect of Cav3 on insulin signaling is stronger than that of Cav1.

A very recent study demonstrated that Cav1KO mice had a primary defect in adipose tissue, as evidenced by drastically reduced IR protein levels (>90%), suggesting that Cav1 is essential for the proper stabilization of the IR protein in adipocytes *in vivo* (15), presumably through the direct binding to IR. Cav1KO mice also showed overt resistance to diet-induced obesity and generalized adipose tissue pathology, especially in old stages (36), suggesting the malfunction of adipocytes. Because Cav3KO mice also showed muscular pathology in old stages (14), it is tempting to speculate that both Cav subtypes play an important role in maintaining the proper phenotype of these tissues. Cav3KO mice, however, did not show reduced IR protein levels or resistance to diet-induced obesity; IR protein expression remained unchanged, and the mice rapidly increased body weight upon high-fat diet (data not shown).

Taken together, Cav subtypes, either Cav1 or Cav3, play an important role in maintaining insulin signaling, even though the mechanism of regulation may differ between the two subtypes. Our transgenic study demonstrated that the role of Cav3 is to maintain neither the protein stability of IR (15) nor its caveolar localization (37) in the skeletal muscle. Instead, as shown by this and a previous study (16), Cav3 enhances insulin signaling at the level of IR$\beta$. Thus, the role of the Cav3 subtype in insulin signaling may be an exception to the common "anchoring and tranquilizing" concept of Cav.

This study was supported in part by grants from the Japanese Ministry of Education, Culture, Sports, Science, and Technology; the Kitsuen Kagaku Research Foundation; and the U.S. Public Health Service (GM067773).

1. Koistinen, H. A. & Zierath, J. R. (2002) *Ann. Med.* **34,** 410–418.
2. Zierath, J. R. & Wallberg-Henriksson, H. (2002) *Ann. N.Y. Acad. Sci.* **967,** 120–134.
3. Smart, E. J., Graf, G. A., McNiven, M. A., Sessa, W. C., Engelman, J. A., Scherer, P. E., Okamoto, T. & Lisanti, M. P. (1999) *Mol. Cell. Biol.* **19,** 7289–7304.
4. Couet, J., Sargiacomo, M. & Lisanti, M. P. (1997) *J. Biol. Chem.* **272,** 30429–30438.
5. Yamamoto, M., Toya, Y., Jensen, R. A. & Ishikawa, Y. (1999) *Exp. Cell Res.* **247,** 380–388.
6. Oka, N., Yamamoto, M., Schwencke, C., Kawabe, J., Ebina, T., Couet, J., Lisanti, M. P. & Ishikawa, Y. (1997) *J. Biol. Chem.* **272,** 33416–33421.
7. Li, S., Couet, J. & Lisanti, M. P. (1996) *J. Biol. Chem.* **271,** 29182–29190.
8. Engelman, J. A., Wykoff, C. C., Yasuhara, S., Song, K. S., Okamoto, T. & Lisanti, M. P. (1997) *J. Biol. Chem.* **272,** 16374–16381.
9. Massimino, M. L., Griffoni, C., Spisni, E., Toni, M. & Tomasi, V. (2002) *Cell Signal.* **14,** 93–98.
10. Peterson, T. E., Guicciardi, M. E., Gulati, R., Kleppe, L. S., Mueske, C. S., Mookadam, M., Sowa, G., Gores, G. J., Sessa, W. C. & Simari, R. D. (2003) *Arterioscler. Thromb. Vasc. Biol.* **23,** 1521–1527.
11. Way, M. & Parton, R. G. (1996) *FEBS Lett.* **378,** 108–112.
12. Song, K. S., Scherer, P. E., Tang, Z., Okamoto, T., Li, S., Chafel, M., Chu, C., Kohtz, D. S. & Lisanti, M. P. (1996) *J. Biol. Chem.* **271,** 15160–15165.
13. Parton, R. G., Way, M., Zorzi, N. & Stang, E. (1997) *J. Cell Biol.* **136,** 137–154.
14. Hagiwara, Y., Sasaoka, T., Araishi, K., Imamura, M., Yorifuji, H., Nonaka, I., Ozawa, E. & Kikuchi, T. (2000) *Hum. Mol. Genet.* **9,** 3047–3054.
15. Cohen, A. W., Razani, B., Wang, X. B., Combs, T. P., Williams, T. M., Scherer, P. E. & Lisanti, M. P. (2003) *Am. J. Physiol.* **285,** C222–C235.
16. Yamamoto, M., Toya, Y., Schwencke, C., Lisanti, M. P., Myers, M. G., Jr., & Ishikawa, Y. (1998) *J. Biol. Chem.* **273,** 26962–26968.
17. Kawabe, J. I., Grant, B. S., Yamamoto, M., Schwencke, C., Okumura, S. & Ishikawa, Y. (2001) *Mol. Cell Endocrinol.* **176,** 91–95.
18. Ueki, K., Yamauchi, T., Tamemoto, H., Tobe, K., Yamamoto-Honda, R., Kaburagi, Y., Akanuma, Y., Yazaki, Y., Aizawa, S., Nagai, R. & Kadowaki, T. (2000) *J. Clin. Invest.* **105,** 1437–1445.
19. Schwencke, C., Yamamoto, M., Okumura, S., Toya, Y., Kim, S. J. & Ishikawa, Y. (1999) *Mol. Endocrinol.* **13,** 1061–1070.
20. Lin, C. Y., Higginbotham, D. A., Judd, R. L. & White, B. D. (2002) *Am. J. Physiol.* **282,** E1084–E1091.
21. Hansen, P. A., Wang, W., Marshall, B. A., Holloszy, J. O. & Mueckler, M. (1998) *J. Biol. Chem.* **273,** 18173–18179.
22. Gulve, E. A., Ren, J. M., Marshall, B. A., Gao, J., Hansen, P. A., Holloszy, J. O. & Mueckler, M. (1994) *J. Biol. Chem.* **269,** 18366–18370.
23. Seta, K., Nanamori, M., Modrall, J. G., Neubig, R. R. & Sadoshima, J. (2002) *J. Biol. Chem.* **277,** 9268–9277.
24. Quantin, B., Perricaudet, L. D., Tajbakhsh, S. & Mandel, J. L. (1992) *Proc. Natl. Acad. Sci. USA* **89,** 2581–2584.
25. Tamemoto, H., Kadowaki, T., Tobe, K., Yagi, T., Sakura, H., Hayakawa, T., Terauchi, Y., Ueki, K., Kaburagi, Y., Satoh, S., *et al.* (1994) *Nature* **372,** 182–186.
26. Bruning, J. C., Michael, M. D., Winnay, J. N., Hayashi, T., Horsch, D., Accili, D., Goodyear, L. J. & Kahn, C. R. (1998) *Mol. Cell* **2,** 559–569.
27. Accili, D., Drago, J., Lee, E. J., Johnson, M. D., Cool, M. H., Salvatore, P., Asico, L. D., Jose, P. A., Taylor, S. I. & Westphal, H. (1996) *Nat. Genet.* **12,** 106–109.
28. Wojtaszewski, J. F., Higaki, Y., Hirshman, M. F., Michael, M. D., Dufresne, S. D., Kahn, C. R. & Goodyear, L. J. (1999) *J. Clin. Invest.* **104,** 1257–1264.
29. Mastick, C. C., Brady, M. J. & Saltiel, A. R. (1995) *J. Cell Biol.* **129,** 1523–1531.
30. Smith, R. M., Harada, S., Smith, J. A., Zhang, S. & Jarett, L. (1998) *Cell Signal.* **10,** 355–362.
31. Gustavsson, J., Parpal, S., Karlsson, M., Ramsing, C., Thorn, H., Borg, M., Lindroth, M., Peterson, K. H., Magnusson, K. E. & Stralfors, P. (1999) *FASEB J.* **13,** 1961–1971.
32. Coderre, L., Kandror, K. V., Vallega, G. & Pilch, P. F. (1995) *J. Biol. Chem.* **270,** 27584–27588.
33. Munoz, P., Mora, S., Sevilla, L., Kaliman, P., Tomas, E., Guma, A., Testar, X., Palacin, M. & Zorzano, A. (1996) *J. Biol. Chem.* **271,** 8133–8139.
34. Hill, M. M., Clark, S. F. & James, D. E. (1997) *Electrophoresis* **18,** 2629–2637.
35. Nystrom, F. H., Chen, H., Cong, L. N., Li, Y. & Quon, M. J. (1999) *Mol. Endocrinol.* **13,** 2013–2024.
36. Razani, B., Combs, T. P., Wang, X. B., Frank, P. G., Park, D. S., Russell, R. G., Li, M., Tang, B., Jelicks, L. A., Scherer, P. E., *et al.* (2002) *J. Biol. Chem.* **277,** 8635–8647.
37. Shankar, R. R., Wu, Y., Shen, H. Q., Zhu, J. S. & Baron, A. D. (2000) *Diabetes* **49,** 684–687.